Available online at www.sciencedirect.com
SCIENCE DIRECT®
Journal of Non-Crystalline Solids 348 (2004) 63–71
JOURNAL OF NON-CRYSTALLINE SOLIDS
www.elsevier.com/locate/jnoncrysol

Optical and structural characterization of rare earth doped niobium phosphate glasses

F.F. Sene, J.R. Martinelli *, L. Gomes

Nuclear and Energy Research Institute, Center of Materials Science and Technology, Av. Lineu Prestes, 2242, Cidade Universitária, CEP 05588-900, Sao Paulo, SP Brazil

Abstract

Phosphate glasses containing up to 45 mol% of niobium were obtained. X-ray diffraction, infrared, Raman, and optical absorption spectroscopy were used to analyze those materials. The refractive index varies from 1.70 to 1.85 as the amount of Nb increases. Niobium phosphate glasses with optical transparence in the (400–2500 nm) range were produced. The cut off varied from 342 nm to 378 nm as a function of the Nb concentration. The cut off is due to the charge transfer $O^2 \rightarrow Nb^{5+}$. Glasses containing 10 mol% of Nb_2O_5 are the most promising materials to be used as rare-earth ions hosts because they are chemically resistant, and show optical transparency in the spectral range of visible to infrared. Doping the glasses with 1–5 mol% of Er, Ho, Pr, and Yb ions does not change the glass structure, as measured by X-ray diffraction, infrared, and Raman spectroscopy. The fluorescence lifetimes were determined for Nd, Yb, and Er, and the absorption cross-section were determined for all ions. The energy transfer in co-doped Yb–Er system was measured, and the lifetime of excited states and the luminescence efficiency were determined to be 91% for the Er $^4I_{11/2}$ level, in the Yb–Er co-doped glasses.

1. Introduction

Oxide glasses are potential hosts for lasers [1]. These lasers can be part of the high-energy (10^3–10^6 J) and high-peak-power (10^{12}–10^{15} W) systems developed for the nuclear fusion reaction tests [2].

The advantage of glasses, in this case, is that large active lasers with good optical quality can be produced. Furthermore, after the development of Nd glass lasers [3], and Nd crystal lasers (Nd:YAG) [4], a search for new solid active lasers using other ions, such as Ho(3+) and Er(3+), that could emit in 2000 and 2700–2900 nm, respectively, began. These ions were investigated in crystal systems, fluoride glasses, and oxide glasses [5]. The energy transfer between rare-earth ions was investigated mainly when they were sensitized by Yb(3+) ions that absorb at 960 nm, which is the wavelength emission of a recently developed high power diode laser [6]. The development of crystal and fluoride glass lasers with Er emitting at 2700 nm is under investigation [7]. The presence of water molecules or absorptions caused by impurities such as OH^-, CHO^- in the region of 4000–3000 cm^{-1}, is responsible for quenching or reduction of the luminescence, preventing their use as active laser host [8].

Oxide glasses doped with Yb(3+) ions can emit at ~1000 nm. They are potentially good for power lasers because they have suitable cross sections for absorption and emission (approximately 2×10^{-20} cm^2) and a spectral width of 30 nm [6]. In crystals and glasses, the Yb(3+) emission band width is larger than in the case of Nd(3+), because Yb(3+) shows an electronic coupling with the host network [6]. An investigation of the luminescence properties of Yb(3+) in phosphate glasses may

* Corresponding author.
E-mail address: jroberto@ipen.br (J.R. Martinelli).

0022-3093/$ - see front matter © 2004 Elsevier B.V. All rights reserved.
doi:10.1016/j.jnoncrysol.2004.08.127

show a potential use of these glasses to generate ultra short pulses.

Phosphate glasses have been investigated as rare-earth ion host matrices in laser systems [9], fibers and optical lenses [10,11]. Phosphate glasses can be produced by melting inorganic precursors at relatively low temperatures (900–1200 °C) and be easily worked [12].

The chemical resistance and transparence of niobium phosphate glasses were investigated to obtain glasses with optical transparency [13]. These glasses are also stable. These characteristics are attributed to O–Nb–O bonds [13]. Other studies using Fourier transformed infrared spectroscopy (FTIR) showed that Nb^{5+} replaces P^{5+}, which is in a tetrahedral coordination in the P–O–P chain. The bridging oxygen is now bonded to Nb^{5+}, forming O–P–O–Nb–O– type chains. It was also shown that P–O type bonds are mostly located in terminal sites of the chain while Nb–O bonds are in the middle sites of the chains [14].

The Raman bands were assigned to O–Nb–O, O–P–O, and mixed O–P–O–Nb–O– chains (named here as PNb) [15]. As the amount of Nb_2O_5 increases, a larger number of Nb–O–Nb and PNb bonds were identified by the Raman spectroscopy [15].

In the present work optical properties and structural properties of niobium phosphate glasses doped with (Pr, Nd, Er, Ho or Yb) ions were investigated. The luminescence lifetime and the absorption cross-section of these ions were also measured.

2. Experimental procedure

Glasses were prepared by mixing different amounts of $(NH_4)_2HPO_4$, Nb_2O_5, KOH, and $BaCO_3$. The molar ratio between phosphorous pentoxide, barium oxide and potassium oxide was kept constant:

$[P_2O_5] = [BaO] = [K_2O] = 1/3$; only the amount of Nb_2O_5 varied.

Table 1 shows the nominal composition of the starting materials produced in this work. The following sample code is adopted: Nb-x, where x is the amount of Nb_2O_5 in mol%.

The batch was melted inside a crucible-type electrical furnace (Lindenberg Blue M). The melting temperature ranged from 1250 to 1350 °C, depending on the composition. The fluid was maintained in the melting temperature for 90 min for homogenization, fining and bubble removal. The liquid was cast into a heated aluminum mold to obtain samples varying in size from $10 \times 10 \times 10\,mm^3$ to $10 \times 10 \times 50\,mm^3$. Cooling gradients, mechanical stresses, and cracks are avoided by using a heated mold. Finally, the material was removed from the mold and annealed in the temperature range of 480–550 °C for 2 h in air, as previously determined for internal stresses release [16].

Table 1
Nominal composition of materials (mol%)

Sample code	$P_2O_5 + BaO + K_2O$	Nb_2O_5
Nb-0	100	0
Nb-5	95	5
Nb-10	90	10
Nb-14	86	14
Nb-19	81	19
Nb-26	74	26
Nb-32	68	32
Nb-37	63	37
Nb-40	60	40
Nb-45	55	45
Nb-50	50	50
Nb-60	40	60

A sample of Nb-10 was selected to host 1–5 mol% of Nd or Yb, and 1 mol% of Er, Pr or Ho. This glass was chosen based on its chemical durability (determined by leaching tests in water at 90 °C), wavelength cut off (determined by optical absorption spectroscopy), and stability (determined by differential thermal analysis) [16].

Slabs 1–4 mm in thickness were cut from glass bars by using a diamond disk saw. These slabs were ground, polished, washed, and finally dried.

Glass powders with average particle sizes of 5 μm were prepared to be used for the X-rays diffraction and Raman spectroscopy.

On bar samples of each composition, the linear refractive index was determined by Snell's law. The incident and refracted angles of a continuous laser with wavelength of 589 nm was measured using a goniometer. The linear refractive index standard deviation was 0.005.

Optical absorption spectroscopy was performed by using a spectrophotometer (*Varian* model *Cary 17D/OLIS)* in the range of 200–2500 nm.

The luminescence life time of the $^4F_{3/2}$ level of the Nd^{3+} for the $^4F_{3/2} \rightarrow {}^4I_{11/2}$ transition, of the $^4I_{13/2}$ level of the Er^{3+} for the $^4I_{13/2} \rightarrow {}^4I_{15/2}$ transition, and of the $^2F_{5/2}$ level of the Yb^{3+} for the $^2F_{5/2} \rightarrow {}^2F_{7/2}$ transition were determined.

The luminescence life time of the $^4I_{13/2}$ of the Er^{3+} for the $^4I_{13/2} \rightarrow {}^4I_{15/2}$ transition, and the life time due to non-radiactive transference of the $^2F_{5/2}$ level of Yb^{3+} to the $^4I_{11/2}$ level of Er^{3+}, and the non-radiative life time assisted by phonons of the $^4I_{11/2}$ level of Er^{3+} were determined for glasses co-doped with Er^{3+} and Yb^{3+}.

3. Results

3.1. Linear refractive index

Fig. 1 shows the linear refractive index (n_0) of phosphate glasses as a function of Nb_2O_5.

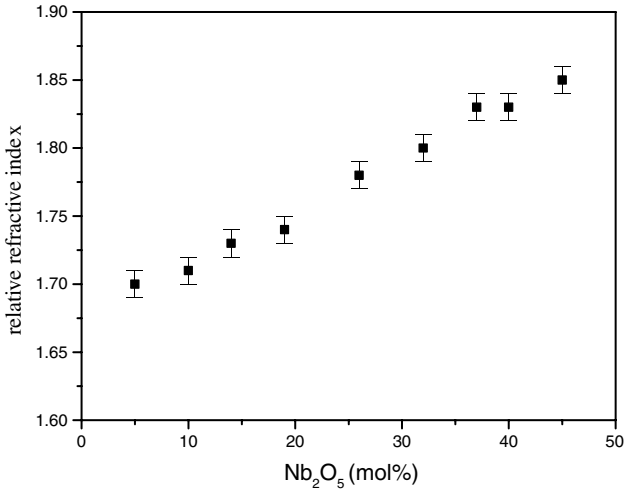

Fig. 1. Linear refractive index of phosphate glass samples as a function of Nb_2O_5 concentration.

3.2. Fourier transform infrared spectroscopy (FTIR)

Fig. 2 shows the FTIR spectra for several niobium phosphate glass samples.

3.3. Raman spectroscopy

Fig. 3 shows the Raman spectra for Nb-10 samples doped with different concentrations of Nd, and with 1 mol% of Ho, Er or Yb, respectively.

3.4. Optical absorption

Fig. 4 shows the optical absorption coefficient as a function of wavelength (λ) for undoped glasses with different amounts of Nb_2O_5. Even though Fig. 4 shows only part of the measured spectra, no absorption bands in the 400–2500 nm were observed in any of these samples.

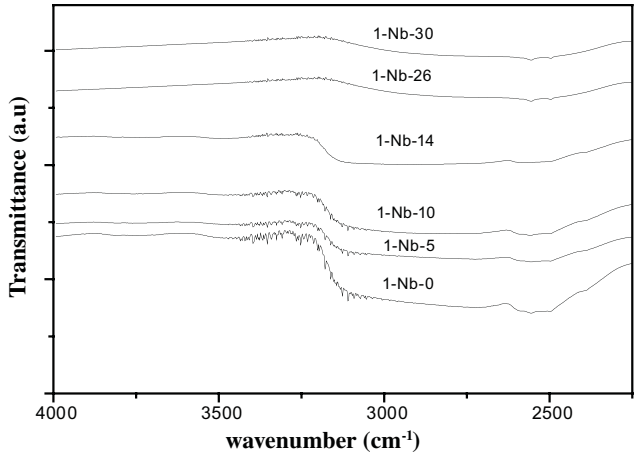

Fig. 2. FTIR spectra of niobium phosphate glass samples with different amounts of Nb_2O_5.

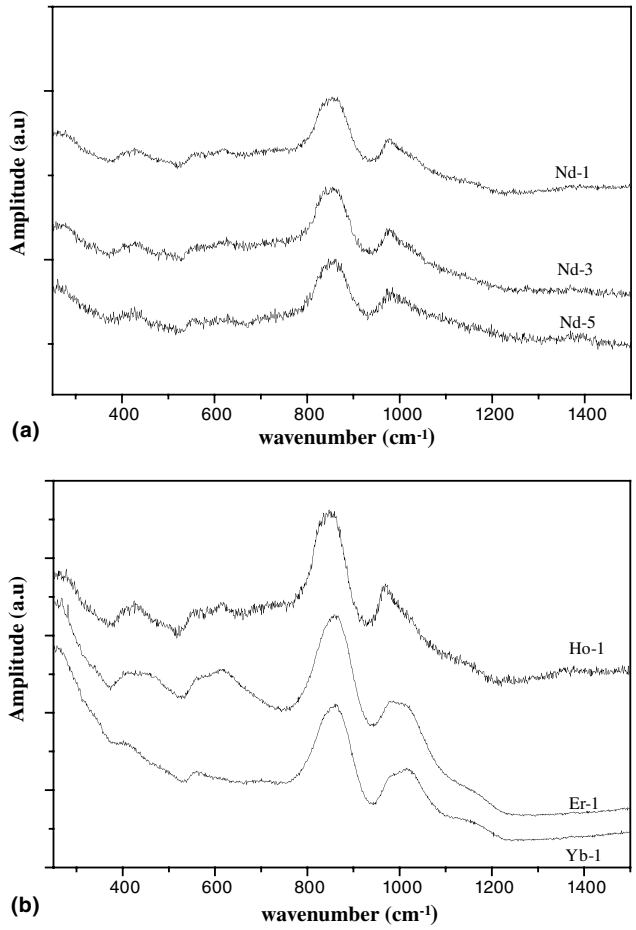

Fig. 3. Raman spectra for Nb-10 doped with: (a) 1, 3, and 5 mol% of Nd, and (b) 1 mol% of Ho, Er or Yb.

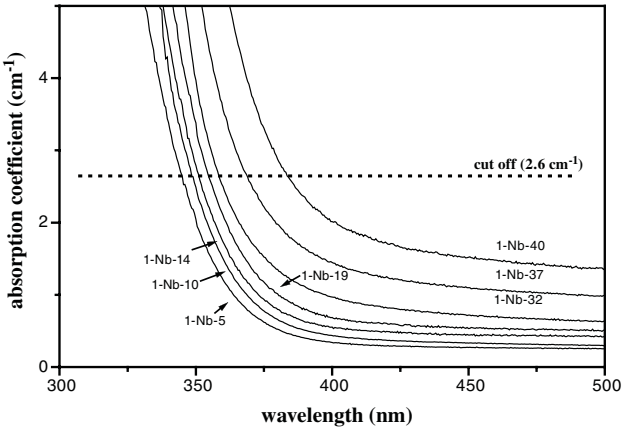

Fig. 4. Optical absorption coefficient of phosphate glass samples with different amounts of Nb_2O_5.

Fig. 5 shows the optical absorption spectra for niobium phosphate glass samples (Nb-10) doped with different concentrations of Nd_2O_3 (1–5 mol%). The detected absorption bands are related to transitions between the electronic levels of Nd.

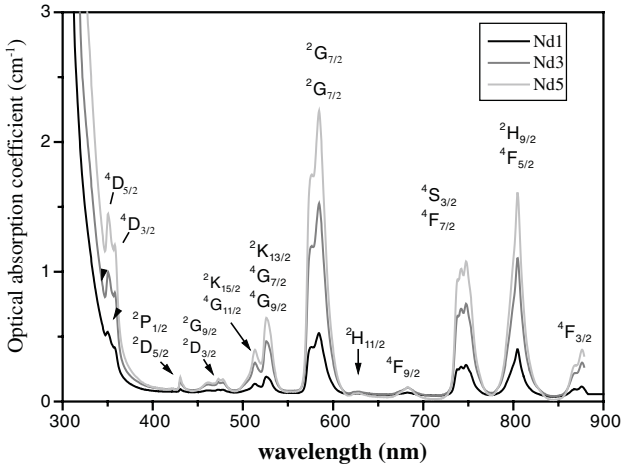

Fig. 5. Optical absorption coefficient of niobium phosphate glass samples doped with 1, 3, and 5 mol% of Nd.

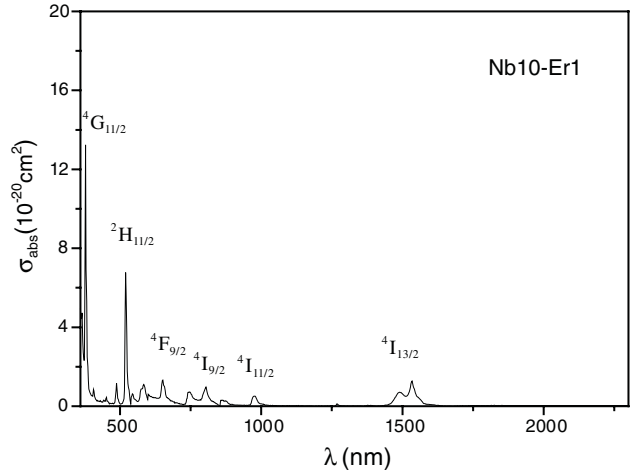

Fig. 7. Absorption cross-section (σ_{abs}) for a niobium phosphate glass sample doped with 1 mol% of Er as a function of wavelength (λ).

Figs. 6–11 show the adsorption cross-section for Nd^{3+}, Er^{3+}, Ho^{3+}, Yb^{3+} and Pr^{3+} ions in niobium phosphate glass samples, respectively.

4. Discussion

From the X-ray diffraction analyses, there is no evidence that crystalline phases are present in samples doped up to 5 mol% with Nd_2O_3. For the Nb-10 glasses doped with 1 mol% of several rare-earth elements, no evidence of crystallization was detected.

The refractive index depends on the electron density or polarizability of ions. Since a majority of the ions in any glass are usually anions [17], the contribution to the refractive index from the oxygen is very important [18]. In the case of undoped glasses, the oxygen is responsible for most of the light refraction [17]. Non-bridging oxygens are strongly polarizable and contribute

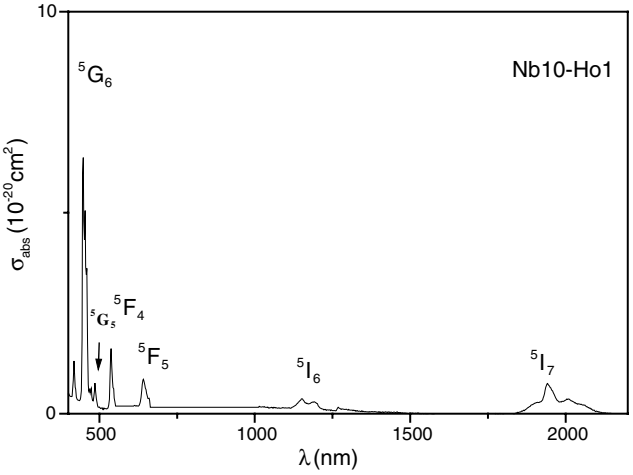

Fig. 8. Absorption cross-section (σ_{abs}) for a niobium phosphate glass sample doped with 1 mol% of Ho as a function of wavelength (λ).

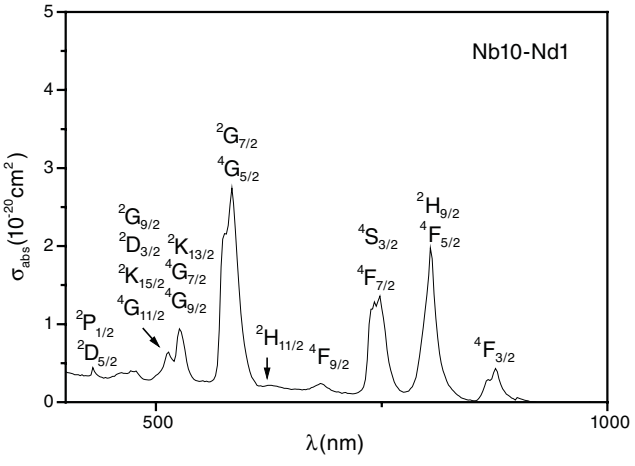

Fig. 6. Absorption cross-section (σ_{abs}) for a niobium phosphate glass sample doped with 1 mol% of Nd as a function of wavelength (λ).

to a larger refractive index. The addition of glass modifiers in phosphate glasses breaks the P–O–P linkages and generates non-bridging oxygens and electrical dipoles that can contribute to an increase of the refractive index [19]. Therefore, different types and amounts of modifiers change the refractive index of glasses. In the present work, the refractive index increases as the amount of Nb_2O_5 increases (Fig. 1). The refractive index also depends on the molar refractive index, density, and glass composition [19]. For phosphate glasses containing M_2O_5 oxides (M = Ta, V or Nb), the linear refractive index increases as a function of the molar fraction of these compounds. This effect is related to the charge of M ions and their coulombian interaction with the coordinated oxygen ions [20]. Even though the determination of the causes related to the refractive index changes in the glass as the amount of niobium oxide increases is

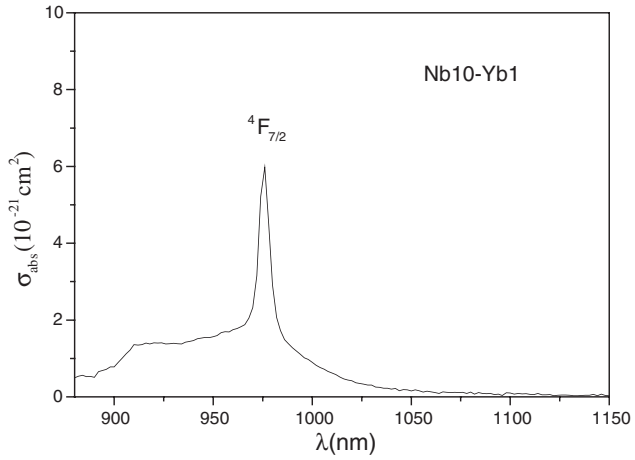

Fig. 9. Absorption cross-section (σ_{abs}) for a niobium phosphate glass sample doped with 1 mol% of Yb as a function of wavelength (λ).

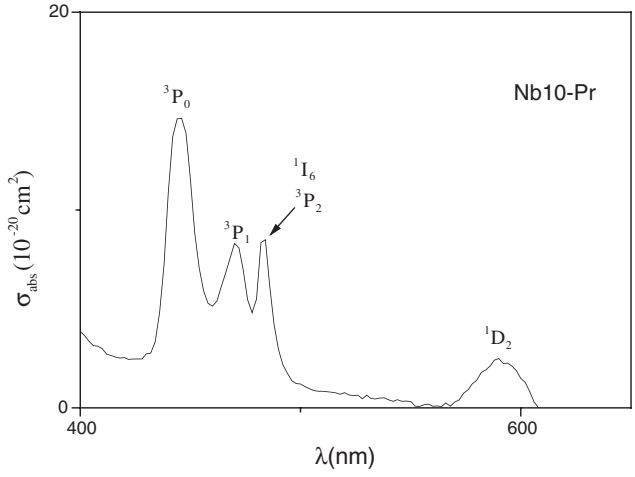

Fig. 10. Absorption cross-section (σ_{abs}) for a niobium phosphate glass sample doped with 1 mol% of Pr as a function of wavelength (λ).

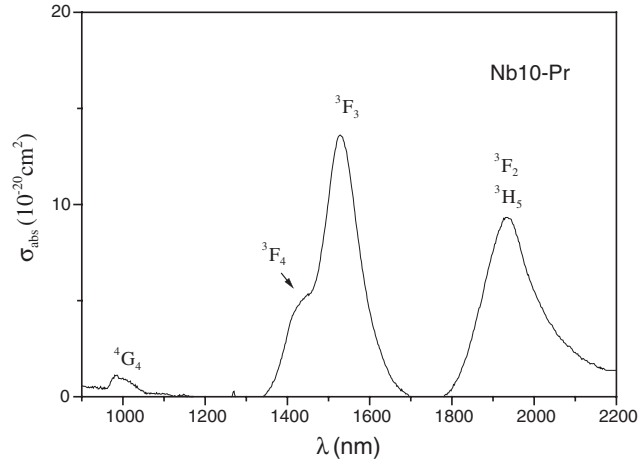

Fig. 11. Absorption cross-section (σ_{abs}) for a niobium phosphate glass sample doped with 1 mol% of Pr as a function of wavelength (λ).

quite complex, the Nb–O linkage leads to an increase of the molecular refractive index, and that depends on the number of Nb–O bonds.

A relatively wide absorption band is observed in the range of 3250–2200 cm^{-1} (Fig. 2) caused by the OH^- [21]. This absorption is reduced as the amount of Nb_2O_5 increases. Therefore, phosphate glasses become less susceptible to the environmental humidity as the amount of niobium is increased.

An absorption band centered at 2370 cm^{-1} (Fig. 2) is assigned to CO_2 (a product from the decomposition of $BaCO_3$ used as raw material in the glass preparation) trapped in the glass structure [22].

An infrared absorption band is resolved between 3450 and 3000 cm^{-1}. This band can be assigned to the presence of water, since this absorption is characteristic of antisymmetric stretching vibrations of free OH groups or free H_2O molecules [23]. The intensity of this band decreases as the amount of Nb_2O_5 increases.

The absorption band centered at 2570 cm^{-1} is assigned to the P–O–H linkages [23], indicating that OH^- is also bonded to P.

Usually the determination of the OH^- concentration requires [21] the knowledge of its molar extinction coefficient (ε). However, in the present work, an alternative method was used, and that is not required.

From the spectra shown in Fig. 2 the absorption coefficients (α) at 3250 cm^{-1} was calculated by using the following equation:

$$\alpha\ (\mathrm{cm}^{-1}) = 2.3026\ \log(1/T)/d, \qquad (1)$$

where T is the transmittance and d is the thickness.

Since water molecules absorb at 3350 cm^{-1} [23], the amount of water molecules was estimated by comparing the determined coefficient with the absorption coefficient previously determined for a water layer [24]. Fig. 12 shows the absorption coefficient of a phosphate glass containing 10 mol% of Nb_2O_5 as a function of the wavenumber. Fig. 13 shows the absorption coefficient of a

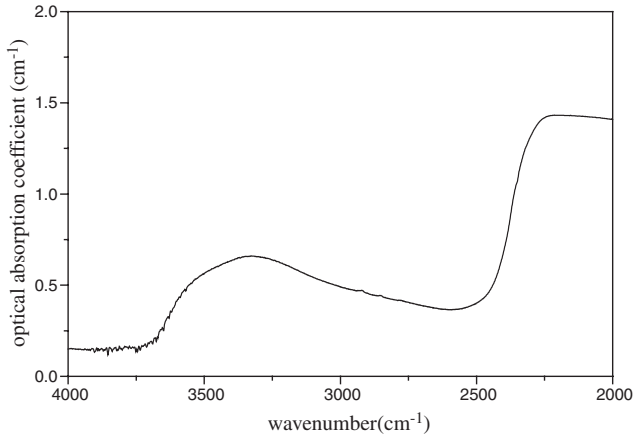

Fig. 12. Optical absorption coefficient of the Nb-10 glass sample.

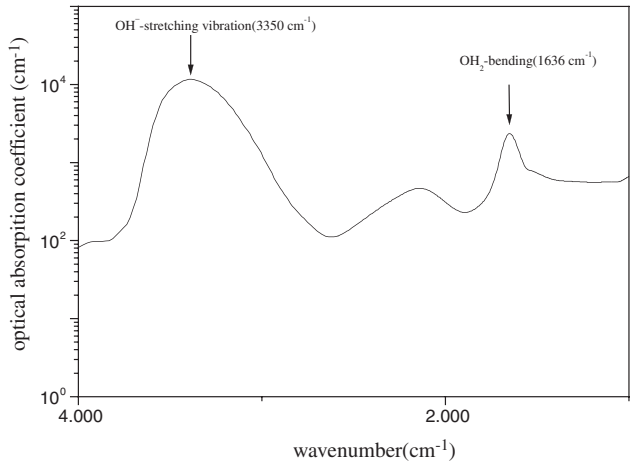

Fig. 13. Optical absorption coefficient for a water layer.

water layer as a function of wavenumber [24]. The absorption coefficient as a function of wavenumber was calculated for glass samples containing 0–30% mol of Nb_2O_5.

Table 2 shows the estimated amount of structural water in the glass as a function of Nb_2O_5 concentration. The detection of structural water is related to absorption due to the stretching of bonded OH^-. The wavenumbers corresponding to the absorption depend on the mass of the neighbor ions and coordination number of the ions in the glass structure. For OH^- groups the absorption occurs between 3250 cm^{-1} and 3600 cm^{-1} [25].

The addition of rare-earth elements in small concentrations do not modify the Raman spectra, and consequently the structure of the host glass, as seen in the Raman spectra of Nb-10 glasses doped with several amounts of Nd (Fig. 3(a)), and with 1 mol% of Ho, Er and Yb (Fig. 3(b)). The same bands previously reported for undoped glasses are observed.

In the present work the molar ratio of barium was kept constant and only the niobium concentration was varied. The absorption coefficient increases as the amount of niobium increases, since the molecular refractive index and density increases. The cut off changes are related to the electronic transitions due to the charge transfer $O^{2-} \rightarrow Nb^{5+}$ [15]. As the amount of Nb is increased, the cut off wavelength will increase. Table 3 shows the cut off wavelength as a function of Nb_2O_5 concentration.

Table 2
Structural OH amount in niobium phosphate glasses as a function of Nb_2O_5 concentration (α is the absorption coefficient at 3350 cm^{-1})

Nb_2O_5 (mol%)	α (cm^{-1})	O_mH_n (10^{-5} mol%)
0	2.066	250
5	1.074	130
10	0.349	40
14	0.165	20
26	0.0661	8
30	0.0413	5

Table 3
Cut off wavelength ($\alpha = 2.6$) as a function of Nb_2O_5 in phosphate glasses

Nb_2O_5 (mol%)	λ cut off (nm)
5	342
10	346
14	348
19	352
32	355
37	364
40	378

It is also noticed that there is an increase of the absorption coefficient as the amount of Nb_2O_5 is increased specially in the visible region of the spectra. This effect is not properly a characteristic of this material but is caused by the light deviation out of the detector range because the incident light beam direction is not normal to the sample surface, and as the linear refractive index of the material increases, this effect becomes more perceptive.

Possible transitions from the $^4I_{9/2}$ to the ground state are indicated in Fig. 5. It can be seen that the absorption in the wavelengths corresponding to the possible transitions increases as the amount of Nd is increased.

Since the absorption cross-section is a parameter that depends on the crystal field of host material, a comparison among different glass systems can give some information concerning the best material to be used as a laser host. Table 4 shows the absorption cross-section for selected glasses, rare-earth ions, and energy levels. In the case of Ho, a crystalline system was referred. Some of the transitions are superposed because the absorption bands are broader in glasses when compared to crystalline systems.

4.1. Luminescence lifetime

The luminescence efficiency, η_{lum}, was calculated from the following equation:

$$\eta_{lum} = \tau/\tau_r, \tag{2}$$

where τ is the experimental lifetime and τ_r is the calculated radiative lifetime.

The radiative lifetime was previously calculated considering an isolated ion [26].

The luminescence lifetime is normally related to τ_r and the non-radiative decay constant, τ_{nr}, as shown below:

$$1/\tau = 1/\tau_r + 1/\tau_{nr}. \tag{3}$$

Figs. 14 and 15 show the luminescence decay curves for $^4F_{3/2} \rightarrow {}^4I_{11/2}$ for niobium phosphate glasses doped with 1 and 3 mol% of Nd. Glasses doped with 5 mol% of Nd

Table 4
Comparison among absorption cross-section of some rare-earth ions in different glasses

Glasses	σ_{abs} (10^{-20} cm^2)				
	Nd (584 nm)	Er (1532 nm)	Ho (1942 nm)	Pr (1530 nm)	Yb (976 nm)
P_2O_5–ZnO_2–Al_2O_3 [15]	3.35				
P_2O_5–K_2O–Li_2O–Al_2O_3 [26]		1.92			
YLF[a] [22]	1.20	0.60	1.55		0.70
GeO_2–PbO–P_2O_5[27]				24.00	
Phosphate glass [28]					0.20
ZBLAN [29]					0.80
Ga_2O_3–Bi_2O_3–PbO [5,30]					2.20
B_2O_3–PbO–PbF_2 [5,30]					2.50
Niobium phosphate glass Nb-10[b]	2.74 ± 0.05	1.23 ± 0.05	0.75 ± 0.05	13.57 ± 0.05	0.59 ± 0.05

[a] Crystal YLF.
[b] This paper.

show similar results. All curves were fitted with exponential functions to allow the determination of the luminescence lifetime.

Fig. 16 shows the luminescence decay curve for the $^4I_{13/2} \rightarrow {}^4I_{15/2}$ transition in niobium phosphate glasses doped with 1 mol% Er. The luminescence efficiency is 57%.

Fig. 17 shows the luminescence decay curve for the $^2F_{5/2} \rightarrow {}^2F_{7/2}$ transition of Yb^{3+} in niobium phosphate glasses doped with 1 mol%. Niobium phosphate glasses doped with 5 mol % of Yb show similar decay curves.

Fig. 18 shows the luminescence decay curve for the $^4I_{13/2} \rightarrow {}^4I_{15/2}$ transition of Er in the niobium phosphate glass. The excitation was done at 930 nm, assuring the absorption by Yb^{3+}. The calculated lifetimes are $\tau_1 = 10\,\mu s$ and $\tau_2 = 6.7$ ms.

Table 5 shows the calculated lifetime for the $^4F_{3/2}$ level from the luminescence decay curve as a function of the Nd concentration and the luminescence efficiency.

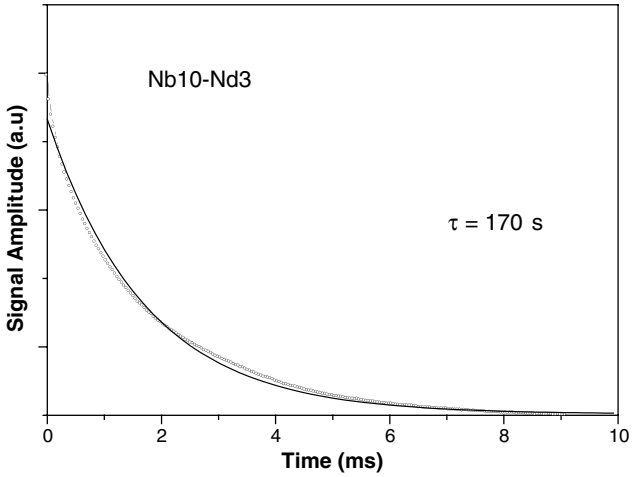

Fig. 15. Luminescence decay curve for the $^4F_{3/2} \rightarrow {}^4I_{11/2}$ transition of the Nd [3 mol%] in niobium phosphate glass sample. The line is the best fit of a exponential decay function. The luminescence lifetime (τ) was determined by the best fitting.

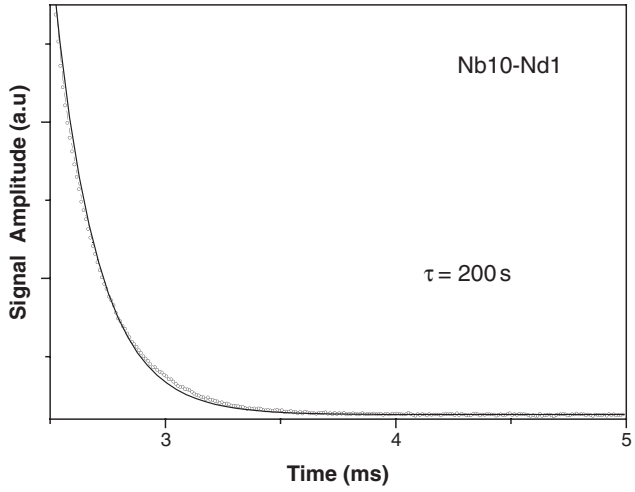

Fig. 14. Luminescence decay curve for the $^4F_{3/2} \rightarrow {}^4I_{11/2}$ transition of the Nd [1 mol%] in niobium phosphate glass. The line is the best fit of a exponential decay function. The luminescence lifetime (τ) was determined by the best fitting.

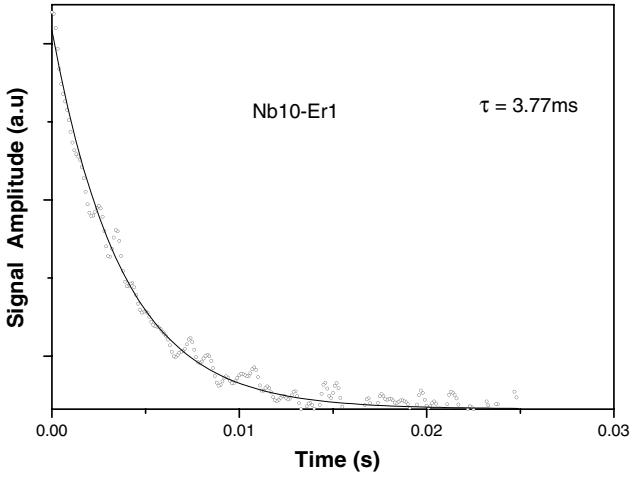

Fig. 16. Luminescence decay curve for the $^4I_{13/2} \rightarrow {}^4I_{15/2}$ transition of the Er [1 mol%] in niobium phosphate glass sample. The line is the best fit of a exponential decay function. The luminescence lifetime (τ) was determined by the best fitting.

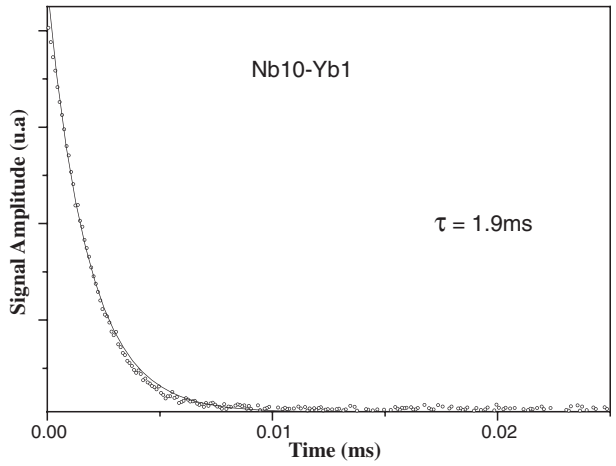

Fig. 17. Lumininescence decay curve for the $^2F_{5/2} \rightarrow {}^2F_{7/2}$ transition for the Nb-10 glass sample doped with 1 mol% of Yb. The line is the best fit of a exponential decay function. The luminescence lifetime (τ) was determined by the best fitting.

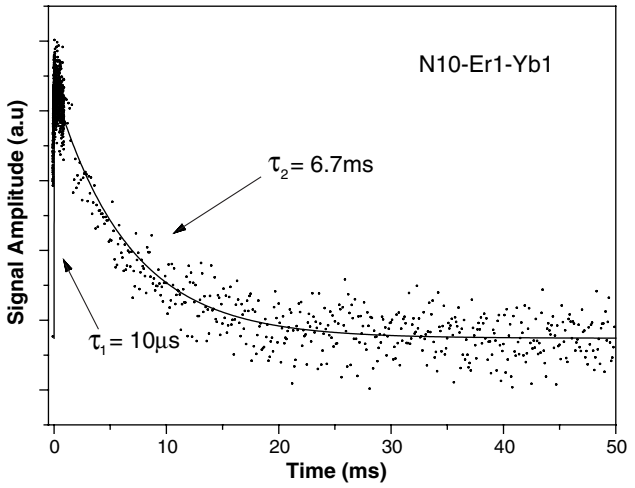

Fig. 18. Luminescence decay curve for the $^4I_{13/2} \rightarrow {}^4I_{15/2}$ transition of Er [1 mol%] in Er–Yb co-doped niobium phosphate glass samples. The line is the best fit of a exponential decay function. The luminescence lifetimes (τ_1 and τ_2) were determined by the best fitting.

Even though glasses doped with 5 mol% of Nd can be easily produced without crystallization, the lifetime of $^4F_{3/2}$ level and the luminescence efficiency decrease as the amount of Nd increases due to cross-relaxation process that occurs through the migration of the excitation between donors when the energy level is identical or through quenching, when the levels are different with same energy. This effect depends strongly on the splitting distance between Nd^{3+} ions, and therefore, the doping concentration. This effect is also noticed for glasses doped with Er (Fig. 16) [27].

Table 5
Luminescence lifetime and efficiency as a function of Nd concentration in niobium phosphate glasses for the $^4F_{3/2}$ level

Nd concentration (mol%)	τ (μs)	η_{lum}
1	200 ± 3	0.38 ± 0.01
3	170 ± 2	0.32 ± 0.01
5	50 ± 2	0.090 ± 0.005

Table 6
Luminescence lifetime for the $^2F_{7/2}$ level in 1% mol Yb doped niobium phosphate glasses

Yb concentration (mol%)	τ(ms)	η_{lum}
1	1.82 ± 0.02	0.80 ± 002
5	1.79 ± 0.02	0.77 ± 0.02

Table 6 shows the calculated luminescence lifetime for the $^2F_{7/2}$ level from the luminescence decay curve and luminescence efficiency as a function of Yb concentration. It is possible to obtain niobium phosphate glasses doped with 5 mol% of Yb without evidence of crystallization. By increasing the amount of Yb no substantial changes in the lifetime of that level is observed because no cross-relaxation process or other non-radiative deactivation mechanism happens [28].

The luminescence lifetime for the 1.5 nm transition was determined for the Nb-10 glass doped with 1 mol% of Er and 1 mol% of Yb.

From the energy diagram of these ions (Fig. 19), it is noticed that Yb absorbs a photon with $\lambda = 930$ nm and an electron is excited to the $^2F_{5/2}$ level with a lifetime τ_1 (10 μs); latter on, this energy is transferred by non-radiactive processes to the Er $^4I_{11/2}$ level at an average time τ_2. The value of τ_2 was determined to be 6.7 ms. The luminescence efficiency determined for this energy level is 0.91. The de-excitation is through two steps: first, a phonon assisted decay to the $^4I_{13/2}$ level, and after that, a photon emission with $\lambda = 1540$ nm with luminescence life time τ_3.

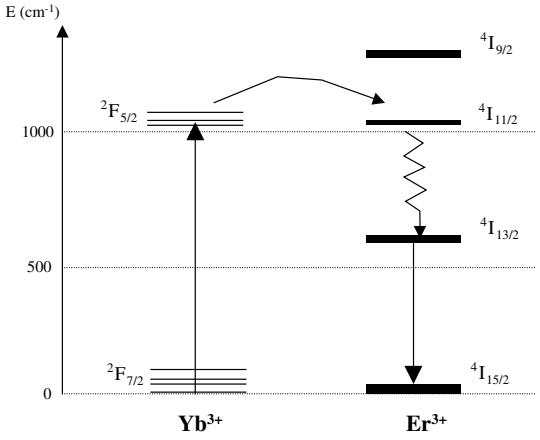

Fig. 19. Energy diagram for Yb and Er. (→ radiative transition, ⇝ non-radiactive transition).

5. Conclusions

Niobium phosphate glasses with optical transparence in the (400–2500 nm) range were produced. The cut off varied from 342 to 378 nm as a function of the Nb concentration. The cut off is due to the charge transfer $O^{2-} \rightarrow Nb^{5+}$.

As the amount of Nb_2O_5 increases, the intensity of a broad absorption band in the range of 3250–2200 cm^{-1} decreases. This band is assigned to the OH^- groups.

The existence of energy transfer in the co-doped Yb–Er in niobium phosphate glass was demonstrated; the lifetime of excited states is 6.7 ms and the luminescence efficiency is 0.91.

A comparison of the absorption cross-section among different glass systems showed that some cross sections determined for niobium phosphate glass samples doped with rare-earth ions, are larger than the ones for other glass types.

Acknowledgment

The authors acknowledge MSc. Fabio H. Jagosich and M.Sc. Andre F. Librantz Schwartz for the optical absorption measurements, Dr Dalva L.A. Faria (University of São Paulo, Chemistry Institute) for the Raman spectroscopy measurements, M.Sc. Hiroshi Oikawa (IPEN) for the infrared spectroscopy measurements. The following funding agencies are also acknowledged: FAPESP Process No. 99/08281-0, FAPESP Process No. 96/9604-9 (XRD analyses), and CNPq (scholarship for F.F. Sene).

References

[1] M.J. Weber, in: 93rd Annual Meeting of the American Ceramic Society, Cincinnati, OH, 1991.
[2] J.H. Campbell, T.I. Suratwala, J. Non-Cryst. Solids 263&264 (2000) 318.
[3] M.J. Weber, J. Non-Cryst. Solids 113 (1990) 206.
[4] J.K. Neeland, V. Evtuhov, Phys. Rev. 156 (2) (1967) 244.
[5] A.A. Kaminskii, Laser Crystals: Their Physics and The Properties, Springer-Verlag, Berlin, 1981.
[6] R. Koch, W.A. Clarkson, D.C. Hanna, S. Jiang, M.J Myers, D. Rhonehouse, S.J. Hamlin, U. Griebner, H. Schönnagel, Opt. Commun. 134 (1997) 175.
[7] J.E. Shelby, Rare elements in glasses, Key Engng. Mater. 94–95 (1994) 175.
[8] A.F. Obaton, J. Bernard, C.G. Le Flem, C. Labbé, P. Le Boulanger, et al., J. Appl. Phys. 4 (1998) 315.
[9] A.H. Khafagy, S.M. ElpRabaie, A.A. Higazy, A.S. Eid, Indian J.Phys. 74A (4) (2000) 433.
[10] B.C. Sales, L.A. Boatner, J. Am. Ceram. Soc. 70 (9) (1987) 615.
[11] W.S. Key and J.C. Miller, Phosphate glass for photonics, in: ORNL Review 27 (3) (1994) 12.
[12] B.S. Sales, L.A. Boatner, Science 226 (1984) 45.
[13] N. Aranha. Niobium Phosphate Glasses: Preparation, Characterization, and Properties, PhD thesis, Unicamp, 1994.
[14] A. El Jazouli, J.C. Viala, C. Parent, G. LeFlem, P.H. Genmuller, J. Solid State Chem. 73 (1988) 433.
[15] A. El Jazouli, R. Brochu, J.C. Viala, R. Ohazcuaga, C. Delmas, G. Le Flem., Ann. Chim. Fr. 7 (1982) 285.
[16] F.F. Sene, Synthesis and Characterization of Niobium Phosphate Glasses Containing Barium and Potassium for Application in Hosting Matrix of Rare-Earth Ions, PhD thesis, USP, 2002.
[17] J.E. Shelby, Introduction to glass science and technology, The Royal Society of Chemistry, 1997, p. 196.
[18] J.E. Shelby, Introduction to Glass Science and Tecnology, The Royal Society of Chemistry, 1997.
[19] J.M.F. Navarro, El Vidreo, Consejo Superior de Investigaciones Científicas, Fundación Centro Nacional del Vidrio, Madrid, España, 1991.
[20] G.A.C.M. Spierings, J. Non-Cryst. Solids 47 (1982) 421.
[21] Y. Abe, D.E. Clerk, J. Mater. Sci. Lett. 9 (1990) 244.
[22] W.M. Pontuschka, M. Sen, C.G. Rouse, Técnicas de preparação de vidros especiais, Graduate course hand-out, IFUSP, 1992.
[23] R.M. Almeida, J.D. Mackenzie, J. Non-Cryst. Solids 40 (1–3) (1980) 535.
[24] F.H. Jagosich, Estudos espectroscópicos para o desenvolvimento dos meios laser ativos de Ho^{3+} e Re^{3+} no YLF, que operam na região de 3 microns, Master thesis, IPEN, 2000.
[25] I.W. Donald, P.W. Mc Millan, J. Mater. Sci. 13 (1978) 1151.
[26] C. Li, Y. Guyout, C. Linarès, R. Moncorgé, M.F. Joubert, OSA Proc. Adv. Solid State Lasers 15 (1993) 91.
[27] M. Ajroud, M. Haouari, H. Ben Quada, H. Maaref, A. Brenier, C. Garapon, J. Phys. Condens. Matter 12 (2000) 3181.
[28] R. Koch, W.A. Clarkson, D.C. Hanna, S. Jiang, M.J. Myers, D. Rhonehouse, S.J. Hamlin, U. Griebner, H. Schönnagel, Opt. Commun. 134 (1997) 175.
[29] P. Goldner, M. Mortier, J. Non-Cryst. Solids 284 (2001) 249.
[30] J.A. Caird, S.A. Payne, Crystalline Paramagnetic Ion Lasers 2-101, in: M.J. Weber (Ed.), Handbook of Laser Science and Technology, CRC Press, Boca Raton, FL, 1991.